Probing Pulsar Dispersion Measures using the GMRT

Amrit Lal Ahuja[1] *, Y. Gupta[2], D. Mitra[2] and A. K. Kembhavi[1]

[1] Inter University Center for Astronomy and Astrophysics, Ganeshkhind, Pune, 411007, India
[2] National Center of Radio Astronomy, Ganeshkhind, Pune, 411007, India

Abstract We present the results from a novel experiment for accurate estimation of pulsar dispersion measure (1 part in 10^4) using the GMRT, without requiring any absolute timing information. The observations were carried out over a period of more than one year for a sample of twelve pulsars. We have used the simultaneous multi-frequency capability of the GMRT. Most of the sample pulsars studied show dispersion measure (DM) variations on time scales of weeks to months. The mean DM value for some of the pulsars show a significant discrepancy with respect to the catalog value. Pulsar B2217+47 shows a large-scale DM gradient over a one year period. For some pulsars we find small differences in the DM values obtained from different frequency combinations.

Key words: miscellaneous — methods: data analysis — pulsars: general — HII regions

1 INTRODUCTION

Due to travel through the ionized inter-stellar medium (ISM), the pulse signals emitted by a pulsar suffer dispersion. The relative time delay Δt (s) in arrival of pulse signals at two frequencies (f_1 & f_2 in MHz) can be expressed as

$$\Delta t \;=\; K \left(\frac{1}{f_1^2} - \frac{1}{f_2^2} \right) \mathrm{DM}\,, \tag{1}$$

where DM (pc cm^{-3}) is the dispersion measure, and the constant $K = \frac{1}{2.410331 \times 10^{-4}}$ MHz^2 cm^3 s pc^{-1}. (Backer et al. 1993). The dispersion measure (DM) of a pulsar needs to be known with sufficient accuracy for proper dispersion correction to be carried out on the received signal, and such accurate estimates are useful to probe the pulsar emission geometry (e.g. Kardashev et al. 1982), to check the validity of the cold plasma dispersion relation for the ISM (e.g. Phillips & Wolszczan 1992 and references therein), and to study the structure of the spectrum of electron density fluctuations (e.g. Backer et al. 1993; Phillips & Wolszczan 1991), etc. The accurate estimates require sophisticated experiments. Here we describe a novel technique for accurate estimation of pulsar DMs, using the GMRT in simultaneous multi-frequency pulsar observation mode, and using Equation 1. The advantage of this method is that a single epoch is self-sufficient for obtaining the DM at that epoch. The subsequent sections describe the details of the observations, data analysis and results & conclusions.

2 OBSERVATION TECHNIQUE

The accuracy of the DM estimate depends on the precision of the estimation of the relative time delay between the pulse profiles at the two frequencies of observation. For a given error in estimation of the time delay (usually limited by the S/N of the data) the greater the Δt, the more accurate is the DM estimate. This would favour large separations between the two observing radio bands. However, the pulse profile evolution with frequency favours a smaller separation between the two radio wave-bands. Also, according

---

to Equation 1, for a given separation between a pair of radio bands, smaller values of frequencies give a larger value of estimated Δt, and in turn, more accurate DM estimation. The final frequency bands of operations were decided by these considerations.

The GMRT is an array of 30 antennas, each of diameter 45 m, distributed over a region of 25 km diameter near Pune, India (for more details see Swarup et al. 1997). This can also be configured as a "single dish" in the incoherent or the phase array mode (see Gupta et al. 2000). The GMRT operates at radio frequency bands 150, 235, 325, 610, and 1400 MHz. The antennas can be grouped into different sub-arrays and all the sub-arrays can be operated simultaneously at different radio band of interest, thus allowing simultaneous multi-frequency observations. Signals from different antennas are eventually down-converted to baseband signals of 16 MHz band-width, and subsequently sampled at the Nyquist rate and processed through a digital receiver system consisting of a correlator and a pulsar back-end. For each antenna, the pulsar back-end receives signals in 256 channels over 16 MHz band-width, for 2 polarisations.

For this experiment, the signals from antennas in all sub-arrays were added incoherently in the same pulsar receiver to produce a single stream of output data, recorded at a sampling rate of 0.516 ms. The relative dispersion delays between the signals at the different radio bands is used to extract the individual de-dispersed data streams at each frequency band (see Ahuja et al. 2005 for details). Our scheme ensures time aligned signals from the different frequency bands, and also does not need absolute time stamps to estimate the delays accurately.

For this experiment, we selected a sample of 12 pulsars having sufficiently large fluxes ($S_{400} > 100 \, \mathrm{mJy}$), a range of DM values ($\sim 10 - 40 \, \mathrm{pc \, cm^{-3}}$), and sampling different directions in the Galaxy. The observations were scheduled almost every fortnight, for 24 hours at each epoch, over a duration of about one and half years. At every epoch of observation, each sample pulsar was observed for a few thousand pulses at a pair of frequency bands of the GMRT (see Ahuja et al. 2005).

3 DATA ANALYSIS

The recorded data were pre-processed off-line, to first carry out the de-dispersion for the two frequency bands, followed by interference rejection. The de-dispersed, interference free data trains were folded at the Doppler-corrected pulsar periods to obtain the average pulse profiles at the two frequency bands (see Figure 1 for an example). The pulse profile data at each observation band were demarcated with three windows − one on-pulse window, containing the properly de-dispersed average pulse profile, and two off-pulse windows (one on each side of the on-pulse) which were centered on off-pulse regions free from wrongly de-dispersed pulse profile of the other frequency band (see Ahuja et al. 2005 for details). Only data from these window regions were used in the subsequent analysis described below.

From the reduced data, the dispersion delay between the two frequency bands was estimated, and using Equation 1, the corresponding DM value was obtained. For the DM calculations, because of the radial velocity of the observer with respect to the pulsar, predominantly due to the orbital motion of the earth around the Sun, the observation frequencies and Δt were Doppler corrected. The total measured time delay, Δt_m, is a sum of three terms: Δt_p, the integral number of pulsar periods delay; Δt_i, the number of time sample bins delay within a pulsar period; and Δt_f, the fraction of a time sample bin delay. We have carried out the analysis by (i) measuring the delay between the average pulse (AP) profiles, and (ii) by measuring the mean delay between the single pulse (SP) data trains.

In the AP method, the value of Δt_p was estimated by using the pulsar catalog DM and period. To estimate Δt_i, pulse profiles at the two frequency bands were cross-correlated, and the integer time sample lag at which the cross-correlation (hereafter CC) peaked was taken as Δt_i. Accordingly, the lower frequency pulse profile was rotated left circularly to align the two pulse profile (see Figure 1). In the SP method, the two time series were cross-correlated. In this method, the CC could be started from zero shift of the lower frequency pulse profile, but to reduce computations, we started CC computations from a shift equivalent to the number of time sample bins corresponding to Δt_p. To estimate the delay with an accuracy of a fraction of a time sample bin, the cross-spectrum (CS) of two aligned pulse profiles was computed, and a linear gradient to the phase of the CS was fitted (see Figure 2) to measure Δt_f. In the AP method, the cross-spectrum obtained from the product of the individual Fourier transformations of the pulse profiles, while in the SP method, it was obtained from the Fourier transformation of the CCF.
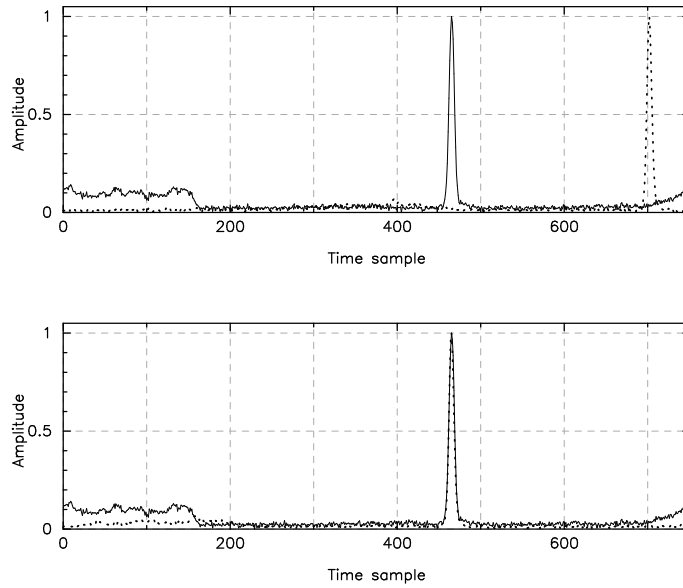
Fig. 1 Average pulse profiles of the PSR B1642−03 observed at 610 (solid curve) + 325 MHz (dotted curve) bands combination, before (upper panel) and after alignment (lower panel).
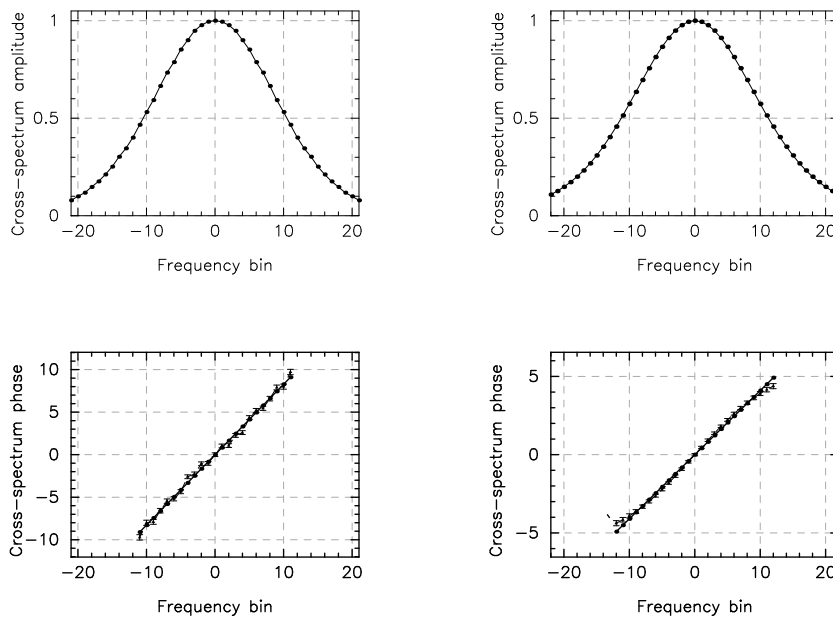
Fig. 2 Normalized CS amplitude (upper panels), and CS phase with error bars (lower panels) of AP (left panels) and SP (right panels) for PSR B1642−03, at one epoch observed at 610+325 MHz bands. The straight line in the phase plot is the best fit linear gradient.

Table 1 DM Results from Average Profile Analysis

Pulsar	Frequency combination (MHz)	Catalog DM (old/new)(pc cm^{-3})	$\langle DM \rangle$ ($\sigma_{DM_{(noise)}}$) (pc cm^{-3})	$\sigma_{DM_{(total)}}$ (pc cm^{-3})	Δ DM / $\sigma_{DM_{(total)}}$ (Old/New)
B0329+54	243 + 610	26.776/26.833	26.77870 (3)	0.00103	+2.64/−52.72
B0818−13	243 + 325	40.99/40.938	40.9222 (13)	0.0043	−15.71/−3.67
B0823+26	243 + 325	19.4751/19.454	19.4545 (4)	0.0016	−12.85/+0.38
B0834+06	243 + 325	12.8579/12.889	12.8671 (4)	0.0017	+5.38/−12.88
B0950+08	325 + 610	2.9702/2.958	2.9597 (8)	0.0050	−2.1/+0.34
B1133+16	325 + 610	4.8471/4.864	4.8288 (6)	0.0071	−2.57/−4.96
B1642−03	325 + 610	35.665/35.727	35.75760 (14)	0.00072	+128.20/+41.67
B1642−03	243 + 325	35.665/35.727	35.72270 (7)	0.00090	+64.00/−4.78
B1919+21	243 + 325	12.4309/12.455	12.4445 (11)	0.0054	+2.50/−1.94
B1929+10	243 + 325	3.176/3.180	3.1755 (4)	0.0015	−0.31/−3.00
B1929+10	325 + 610	3.176/3.180	3.1750 (4)	0.0020	−0.51/−2.50
B2016+28	243 + 320	14.176/14.172	14.1611 (7)	0.0025	−6.07/−4.36
B2016+28	325 + 610	14.176/14.172	14.1664 (8)	0.0051	−1.90/−1.10
B2045−16	243 + 320	11.51/11.456	11.5094 (12)	0.0114	−0.05/+4.68
B2217+47	325 + 610	43.54/43.519	43.5196 (7)	0.0061	−3.38/+0.86
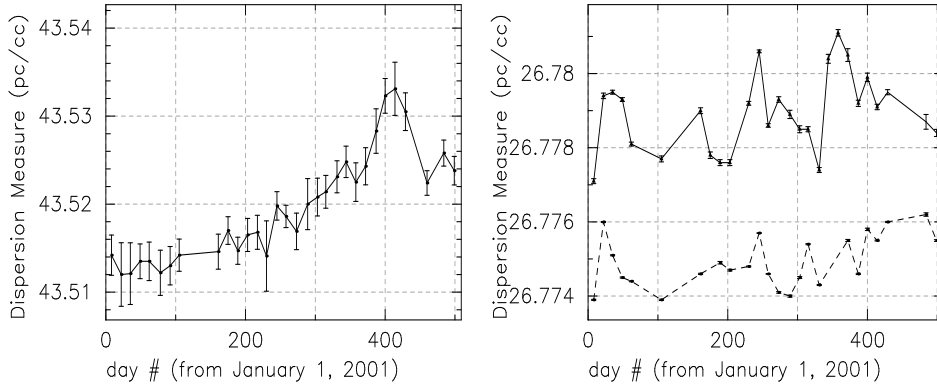
Fig. 3 Variation of DM with time for pulsars B2217+47 (left panel) and B0329+54 (right panel) respectively. In the right panel, continuous line shows the results from AP analysis, and the dotted one from SP pulse analysis. The error bars are $3\sigma_{DM_{(noise)}}$ values.

For the AP method, the noise in the folded profiles, estimated from the off-pulse windows, was properly propagated to the CS. In the SP method, the RMS obtained from off-pulse windows was properly propagated to estimate the RMS at each point of the CCF. The greatest value of this RMS was used as an estimate to the RMS of the CS phase. By using the three components of measured time delay, DM was estimated at each epoch. The above steps were carried out at at all the epochs to obtain a time series of DM values for each pulsar (see Figure 3). For more details, see Ahuja et al. 2005.

4 RESULTS AND CONCLUSIONS

The results obtained for the average profile method are summarised in Table 1. Here, column 2 gives the observing frequency bands and column 3 tabulates the old and new catalog DM values from Taylor, Manchester, & Lyne 1993 and Hobbs et al. 2004, respectively. For each pulsar, we obtained the mean DM over the period of observations ($\sim$ 30 epochs), $\langle DM \rangle$, and the quadrature average of the quantity $\sigma_{DM_{(noise)}}$ (column 4 of Table 1), an estimate of a source error in the DM estimation. The values of $\sigma_{DM_{(noise)}}$ for most of the sample pulsars are 1 part in 10^4 or better. The total fluctuation of the DM time

series, $\sigma_{\mathrm{DM_{(total)}}}$ (column 5 of Table 1), is composed of a part due to estimation error on the DM, and the remaining due to other variability processes like DM fluctuation due to large scale electron density irregularities in the ISM. Keeping in mind the $\sigma_{\mathrm{DM_{(total)}}}$, the $\langle\mathrm{DM}\rangle$ for each pulsar is estimated with a fairly good accuracy: ~ 1 part in 10^3 or better (DM accuracy at each epoch is ~ 1 part in 10^4).

Column 6 of Table 1 shows the ratio between our $\langle\mathrm{DM}\rangle$ value and the catalog (Old/New) DM value (Taylor, Manchester, & Lyne 1993; Hobbs et al. 2004), in units of $\sigma_{\mathrm{DM_{(total)}}}$. While for most pulsars our results agree with the catalog values within $3\,\sigma_{\mathrm{DM_{(total)}}}$, there are some pulsars, which show a significant difference. Amongst all our results, the mean value of DM for PSR B1642$-$03 shows the largest discrepancy with the original catalog value of $35.665(5)$ pc cm^{-3} (based on very early work of Hunt 1971). The new pulsar catalog gives a value of $35.727(3)$ pc cm^{-3} (Hobbs et al. 2004), which is close to the lower of our two results.

For two of our pulsars – B1642$-$03 and B2016+28 – we carried out the observations at two pairs of frequency bands. PSR B1642$-$03 shows significant difference in the mean DM values from the two sets of data (Table 1). On the other hand, for B2016+28 the DMs obtained from the two frequency pairs are the same within errors. Such DM variations with frequency are reported earlier also (e.g. Shitov et al. 1988; Hankins 1991). Some of these variations can be explained due to pulse profile evolution with frequency. Another interesting possibility is an extra time delay due to the emission originating at different heights in the magnetosphere. We are studying some of these possibilities, with the help of numerical simulations.

As described in section 3, the DM estimates were obtained in two different ways: the AP and the SP methods. For some pulsars, the DM difference obtained from the two methods, is significant, e.g., PSR B0329+54 (see Figure 3) – the $\langle\mathrm{DM}\rangle$ value obtained from the SP analysis is $26.7751(7)$ pc cm^{-3}. This aspect of our results needs to be investigated further.

There is evidence for substantial temporal fluctuations in DM values for most of the pulsars. Most of our observed DM fluctuations (except PSR B2217+47) show fluctuations around a relatively constant mean DM, indicating that the observed changes are likely to be due to electron density fluctuations in the ISM. However, PSR B2217+47 shows an almost monotonic increase of its DM (Figure 3). A likely cause for this change is that the pulsar is sampling an electron density gradient in the ISM, possibly produced by the line of sight to the pulsar crossing through a blob of enhanced plasma density (see Ahuja et al. 2005 for a detailed explanation).

References

Ahuja, A. L., Gupta, Y., Mitra, D., Kembhavi, A. K., 2005, MNRAS, 357, 1013

Backer, D. C., Hama, S., Hook, S. V., Foster, R. S., 1993, ApJ, 404, 636

Gupta, Y., Gothoskar, P. B., Joshi, B. C., Vivekanand, M., Swain, R., Sirothia, S., Bhat, N.D.R., 2000, in IAU Colloq. 177, Pulsar Astronomy, ed. M. Kramer, N. Wex, And R. Wielebinski (ASP Conf. Ser. 202; San Francisco: ASP), p.277

Hankins, T.H., 1987, ApJ, 312, 276

Hankins, T. H., Izvekova, V. A., Malofeev, V. M., Rankin, J. M., Shitov, Y. P., Stinebring, D. R., 1991, ApJ, 373, L17

Hobbs, G., Lyne, A. G., Kramer, M., Martin, C. E., Jordan, C. A., 2004, MNRAS, 353, 1311

Hunt, G. C., 1971, MNRAS, 153, 119

Kardashev, N. S., Nikolaev, N. Ya., Novikov, A. Yu., Popov, M. V., Soglasnov, V. A., Kuzmin, A. D., Smirnova, T. V., Bartel, N., Sieber, W., Wielebinski, R., 1982, A&A, 109, 340

Phillips, J. A., Wolszczan, A., 1991, ApJ, 382, L27

Phillips, J. A., Wolszczan, A., 1992, ApJ, 385, 273

Shitov, Yu. P., Malofeev, V. M., Izvekova, V. A., 1988, Sov. Astron. Lett., 14(3), 181 and Kaspi, V. M., 1992, in IAU Colloq. 128, ed. Hankins, T.H., Rankin, J.M., Gil, J.A., (Poland: Padagogical University Press), p.349

Swarup, G., Ananthakrishnan, S., Subrahmanya, C. R., Rao, A. P., Kulkarni, V. K., Kapahi, V. K., 1997, in High Sensitivity Radio Astronomy, ed. N. Jackson, R. J. Davis (Cambridge: Cambridge University Press)

Taylor, J. H., Manchester, R. N., Lyne, A. G., 1993, ApJS, 88, 529